Jusami
Jurnal Sains Materi Indonesia
Homepage: http://jusami.batan.go.id
Akreditation No : 21/E/KPT/2018
Date 9 July 2018
ISSN 1411-1098
E-ISSN 2614-087X

SYNTHESIS OF MAGNETIC COMPOSITE OF IRON COMPOUNDS/CARBON NANOTUBES IN CHEMICAL VAPOR DEPOSITION

Teguh Endah Saraswati[1], Oktaviana Dewi Indah Prasiwi[1], Abu Masykur[1] and Miftahul Anwar[2]

[1] Department of Chemistry, Sebelas Maret University
Jl. Ir. Sutami 36 A Surakarta 57126 Indonesia
[2] Department of Electrical Engineering, Sebelas Maret University
Jl. Ir. Sutami 36 A Surakarta 57126 Indonesia
E-mail: teguh@mipa.uns.ac.id

Received: 29 November 2018 *Revised: 25 March 2019* *Accepted: 29 March 2019*

ABSTRACT

SYNTHESIS OF MAGNETIC COMPOSITE OF IRON COMPOUNDS/CARBON NANOTUBES IN CHEMICAL VAPOR DEPOSITION. The chemical vapor deposition (CVD) synthesis of magnetic composite of iron compounds/carbon nanotubes (com-CNT) has been successfully carried out in various pressures using a catalyst of iron oxide/carbon. The temperatures were set at 800° C for 10 minutes reaction time. Nitrogen (N_2) gas in 20 Torr was flown in followed by ethanol vapor until the final pressure reached 80 and 100 Torr without added air, and 180 Torr with added air. The formation of com-CNT was confirmed by shifted X-ray diffraction (XRD) peak of graphite from 26.53° to 25.53° which were highly considered to the other carbon allotropes with sp^2 hybridized carbon atom hybridization structures. The higher pressure with added atmospheric air led to the excessive oxidation which influenced the growth of com-CNT. Transmission electron microscopy (TEM) analysis observed CNT filled by catalyst particles which suggested as magnetic phase induced the magnetic property of com-CNT. The magnetic property of the composites was roughly estimated by observing the attraction of com-CNT toward a permanent magnet. The rough value of the lowest electrical resistance was owned by com-CNT produced in the lower pressure condition with no air added.

Keywords: Carbon nanotubes, Chemical vapor deposition, Catalyst, Magnetic, Iron oxide

ABSTRAK

SINTESIS KOMPOSIT MAGNETIK SENYAWAAN BESI/*CARBON NANOTUBE* DENGAN *CHEMICAL VAPOR DEPOSITION*. Sintesis komposit magnetik senyawaan besi/*carbon nanotube* (com-CNT) dengan chemical vapor deposition (CVD) telah berhasil dilakukan dalam variasi kondisi tekanan menggunakan katalis besi oksida/karbon. Kondisi sintesis dilakukan pada 800 °C selama 10 menit waktu reaksi. Gas nitrogen (N_2) dengan tekanan 20 Torr dialirkan ke dalam *chamber* vakum diikuti oleh uap etanol hingga mencapai tekanan akhir sebesar 80 dan 100 Torr, keduanya tanpa tambahan udara, dan 180 Torr dengan tambahan udara. Pembentukan com-CNT dikonfirmasi oleh pergeseran difraksi sinar-X (XRD) puncak grafit dari 26,53 ° ke 25,53 ° yang mengindikasikan pula pada pembentukan alotrop karbon lainnya yang memiliki struktur dengan atom karbon terhibridisasi sp^2. Tekanan yang lebih tinggi dengan penambahan udara menyebabkan oksidasi berlebih yang mempengaruhi pertumbuhan com-CNT. Analisis struktur partikel dengan menggunakan mikroskop elektron transmisi (TEM) berhasil mengamati com-CNT terisi oleh partikel katalis yang bertanggungjawab pada munculnya sifat magnetik pada com-CNT yang terbentuk. Sifat magnetik komposit ditunjukkan secara kasar dengan melihat ketertarikanmaterial com-CNT dengan magnet permanen. Nilai kasar resistansi listrik yang paling rendah dimiliki oleh com-CNT yang diproduksi dalam kondisi tekanan rendah tanpa tambahan udara.

Kata kunci: *Carbon nantotube, Chemical vapor deposition,* Katalis, Magnetic, Besi oksida

INTRODUCTION

In recent years, carbon-based nanomaterials have been widely studied and developed because they can be applied in various fields. One of the carbon-based nanomaterials currently being developed is carbon nanotubes (CNT), which were first discovered by Iijima in 1991 in the form of hexagonal carbon neatly arranged and shaped like a pipe [1]. CNT has good heat and electrical conductivity, small band gap energy, and good mechanical strength, therefore, they are applicable across different fields. Some examples of CNT applications include ceramic composites [2], anode materials on lithium batteries [3], and conductive materials [4].

There are various CNT synthesis methods, including arc discharge [5], chemical vapor deposition (CVD) [6], plasma enhanced chemical vapor deposition (PE-CVD) [7,8], pyrolysis [9], and laser ablation [4]. Each method has advantages and disadvantages. The CVD method is often used because it is a simple, economical process with a low impurity level [10]. CNT synthesis by CVD can also be carried out at low temperatures and ambient pressures [11].

The use of the CVD method requires a catalyst to produce carbon nanotubes—such as commonly used metal catalysts, including nickel (Ni) [12,13], cobalt (Co) [14,15], iron (Fe) [16], or a dual transition metal (Fe-Co) on supporting material like zeolite [17] and silicon (Si) [18]. However, because of its abundance and ease of access, Fe may be the most preferred CVD catalyst. It induces the magnetic property of the product and produces greater yields of CNT than does Co [19]. However, Fe powder is oxidized when it reacts with oxygen in the air at high temperatures, where its oxide phase is also more easily available. Choi et al. (2011) performed CNT synthesis using the pyrolysis method carried out with an Fe_2O_3/carbon catalyst [9]. The reduction process of the catalyst during CVD is required to activate the catalytic property, usually performed by hydrogen gas.

Modifications of CNT that are currently interesting to study are magnetic carbon nanotubes. Some applications of magnetic CNT include magnetic storage [20], spintronics [21], and biomanipulation [22]. The preparation of magnetic CNT, as reported by pioneering works, is commonly performed in separated steps, i.e., CNT synthesis by CVD followed by different methods, such as hydrothermal [23], co-precipitation [24-26], thermal decomposition, solvothermal [27,28], sol-gel [20,29], and pyrolysis [30].

Korneva et al. (2005) have modified magnetic CNT by inserting magnetic particles into the CNT [31]. They used magnetic material, in the form of Fe_3O_4, by opening the tip structure of the CNT to be filled with magnetic particles. However, this modification process is less efficient because it is performed in multiple steps, i.e., CNT synthesis followed by the modification. Therefore, synthesizing magnetic CNT in one step will be more efficient. A single step of magnetic CNT synthesis may possibly be directly by CVD, as reported in several articles [32-34]. However, in this single step, the high purity of hydrocarbon gases (e.g., methane, acetylene, propane, etc.) mixed with hydrogen and inert gases is still required to produce the CNT, which causes higher production costs. Therefore, a single stage com-CNT synthesis that avoids using expensive gases is desired.

Considering that CVD uses a catalyst, carbon-based nanoparticles could possibly be used in CVD to act as both a catalyst and a replacement for the carbon source commonly provided by hydrocarbon gas. During the CVD process, the metal or metal oxide contained in this proposed catalyst would activate the surrounding carbon to grow and form the CNT structure. Bekarevich et al. (2012) successfully carried out PE-CVD CNT synthesis with a Ni/carbon nanomaterial catalyst resulting from arc discharge fabrication [35]. Similarly, this present study reports magnetic composite of iron compounds/carbon nanotubes (com-CNT) synthesis via the CVD method using a magnetic iron oxide-(Fe_3O_4)/carbon catalyst in core-shell structure, which was intended to play the role of both catalyst and carbon source. Moreover, we investigated com-CNT growth in three separate experimental conditions of a various total gas pressure of N_2 and ethanol vapors with and without air addition. The introduction of ethanol vapor and air during the CVD process were designed to initiate the opening of the carbon shell of catalyst via oxidation reaction. However, the various pressure conditions resulted in different products which are quite interesting to be discussed.

EXPERIMENTAL METHOD

Materials

The materials used in this experiment were a nanocomposite of Fe_3O_4/carbon catalyst in size of ~20 nm, prepared by submerged arc discharge [36]; distilled water; ethanol (99%) (Merck); graphite powder (Merck); commercial silica binder; and carbon electrodes (Qingdao Tennry Carbon Co., Ltd.). The gas used in this experiment was N_2 gas (PT. Samator Gas Industri, UHP grade).

Method and Procedure

The synthesis process in CVD

The com-CNT synthesis was carried out via the CVD method, using an Fe_3O_4/carbon catalyst. The experimental setup of the CVD chamber (shown in Figure 1) consisted of a quartz tube with a diameter of 60 mm in a horizontal furnace that was connected to an inlet gas hose and an exit gas (vacuum) hose. The left and right of the quartz tube were cooled to reduce

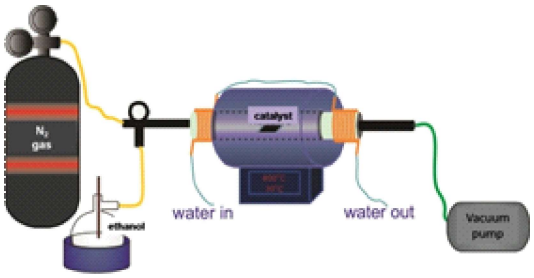

Figure 1. The experimental setup of chemical vapor deposition (CVD).

the significant temperature gap with the heated quartz zone.

The metal plate in size of 10 x 10 mm, coated with the catalyst, was placed in the middle of the quartz tube. The tube was vacuumed for ten minutes until the pressure in the tube was stable and was below 1 atm. Nitrogen gas flowed into the tube for five minutes to remove water vapor and other vapor impurities from the tube. The vacuum was then closed, and nitrogen gas flowed in until the tube pressure reached 20 Torr pressure followed. Ethanol vapor followed the nitrogen, until the final pressure reached, in three separate experiment variations, 80, 100 and 180 Torr pressure. In all variations, the furnace was turned on after the target Torr pressure was reached, and the temperature was set to 800°C for ten min. Then, the furnace was turned off, and the temperature was gradually decreased to room temperature before the sample was taken out. In the latter variation condition, the pressure was gradually increased by flowing atmospheric air inside until the pressure reached atmospheric pressure. The introduced ethanol vapor and the air were intended to oxidize the excess of amorphous carbon material.

The com-CNT resulting from this Fe_3O_4/carbon catalyst were characterized using an X-ray diffractometer (XRD, Bruker D8 Advance) and a transmission electron microscope (TEM, JEOL JEM-1400). The com-CNT magnetic properties were roughly measured by observing the interaction of the com-CNT with a permanent magnet. The electrical resistance of the com-CNT was estimated at room temperature by a method previously reported by Celzard et al. [37] with modification and was roughly measured using a inductance (L), capacitance (C), and resistance (R) meter (LCR digital multimeter).

RESULT AND DISCUSSION

To confirm the material structure and crystallinity, the diffraction patterns of the materials were analyzed using XRD, as shown in Figure 2. In addition, we presented a diffraction spectrum of commercial CNT as a comparison shown in Figure 2(a). The XRD profiles of the Fe_3O_4/carbon catalyst, prepared in submerged arc discharge, and com-CNT synthesized in three different conditions are shown in Figures 2(b) through 2(e). The structure and properties of the prepared catalyst were discussed in our previous publication [36,38]. Figures 2(c) through 2(e) show the XRD profiles of the CNT produced in different pressure and gas conditions: 80 Torr and 100 Torr, without atmospheric air addition; 180 Torr, with atmospheric air addition.

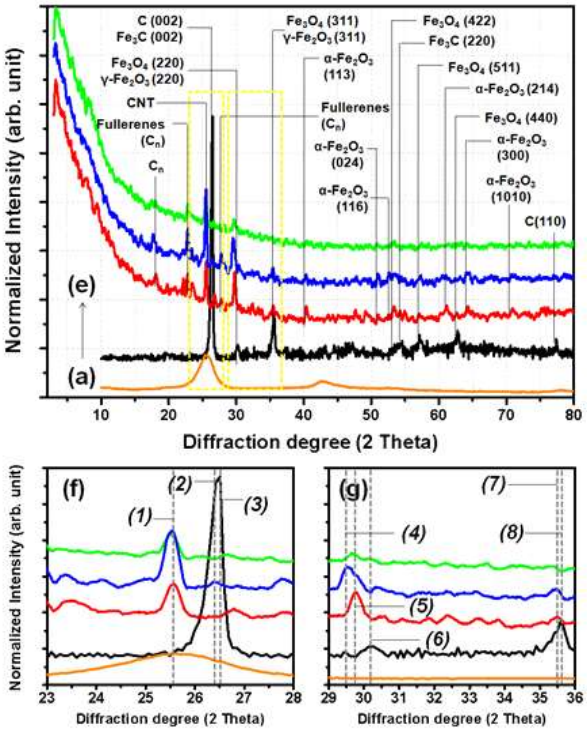

Figure 2. XRD profiles of (a). commercial CNT; (b). catalyst, CNT produced in different pressure and gas conditions; (c). 180 Torr with atmospheric air addition; (d) 100 Torr without atmospheric air addition; and (e). 80 Torr without atmospheric air addition; (f). and (g). the emphasized dashed yellow regions. The corresponded dashes line numbers (1) to (8) were presented in detail in Table 1.

To provide the satisfied discussion, we added the crystallographic spectra emphasized from the area in the yellow dashed line of a wider spectra as shown in Figure 2(f) and (g). In addition, we added the detail information showing the 2-theta diffraction peaks inside Figure 2(g) as presented in Table 1. For analysis, the XRD profiles were compared to the diffraction database of carbon graphite (#PDF 41-1487), Fe_3C (#PDF.85-0871), α-Fe_2O_3 (#PDF 85-0597), fullerenes C_{70} (#PDF 48-1206), Fe_3O_4 (#PDF 75-0449), and γ-Fe_2O_3 (#PDF 39-1346).

After CVD treatment, the represented graphite peak, which normally appears at 2θ around 26°, according to C(002), has undergone a leftward shift. This peak shifting indicates that the spacing distance between graphene sheets of 0.34 nm, as observed in the C(002) diffraction peak of the initial catalyst as shown in Figure 2(b), could not be maintained after CVD processing. The emphasized crystallographic spectra presented in Figure 2(f) are in agreement with previous works [39,40] in which the peak of C(002) was also broad and had shifted. This

Table 1. The resolution of the diffraction peaks (2θ) 29-26° of material before and after CVD treatment compared to powder diffraction file (PDF) database of γ-Fe_2O_3 and Fe_3O_4.

Lattice planes (hkl)	Diffraction peaks (2θ) (Note: the number in square bracket correspond to the dashed line number in Figure 2(g))					
	Before CVD (catalyst alone)	After CVD treatment			γ-Fe_2O_3 PDF# 39-1346	Fe_3O_4 PDF# 89-0691
		80 torr without air addition	100 torr without air addition	180 torr with air addition		
(220)	30.20 *(6)*	29.63 *(5)*	29.52 *(4)*	29.76 *(5)*	30.27	30.36
(311)	35.58 *(8)*	-	35.47 *(7)*	35.49 *(7)*	35.66	35.77

phenomenon strongly suggests that CNT have been successfully synthesized. The broadener and shifted characteristic at ~26° is also in agreement with the spectra of commercial CNT as shown in Figure 2(a).

The presence of other diffraction peaks in the range of 15° " 80° corresponded to the remaining catalyst, and amorphous carbon compounds still existed in the synthesized material. These additional peaks were confirmed belonging to iron carbides and iron oxide, including γ-Fe_2O_3 and Fe_3O_4, which were observed in the XRD spectra of all synthesized materials. The existence of these iron oxide phases acted as the magnetic phase, inducing the magnetic property of the com-CNT products.

As shown in Figure 2, according to the diffraction database of Fe_3O_4 (#PDF 75-0449), and γ-Fe_2O_3 (#PDF 39-1346), the observable peaks correspond to the crystalline planes of (220), (311), (422), (511), and (440)—belonging to magnetite (Fe_3O_4) and maghemite (γ-Fe_2O_3). The pattern assignment of Fe_3O_4 and γ-Fe_2O_3 was difficult to resolve because they showed similar electron diffraction and X-ray diffraction patterns [41]. Both of magnetite and maghemite phases have the spinel structure and lattice parameter, thus the diffraction peaks are located adjacent to each other. As presented in the emphasized spectra in Figure 2(g), Fe_3O_4 and γ-Fe_2O_3 have very close diffraction peaks.

In detail, according to the diffraction database #PDF 75-0449 and PDF 39-1346, Table 1 presents that the lattice plane (220) of Fe_3O_4 and γ-Fe_2O_3 reveals at 30.36° and 30.27°, respectively. Meanwhile, the lattice plane (311) of Fe_3O_4 and γ-Fe_2O_3 appears at 35.77° and 35.66°, respectively. However, after the CVD treatment, the diffraction peaks of the catalyst shifted from 2θ of 30.20 and ~29 (for (220) lattice plane) and from 2θ of 35.6 and ~35.4 (for (311) lattice plane). These shifting peaks indicated to the expanding of the lattice structure and the lattice distance. Moreover, the peak shifting was significantly observable for the material treated with oxygen-rich treatment conditions (i.e., with air addition) which supposedly occurred due to the insertion of more oxygen into the crystalline of Fe_3O_4 and γ-Fe_2O_3.

After CVD treatment, beside the peak shifting, some new peaks appear at 2θ = 40.47°, 50.72°, and 53.6° correspond to the crystalline planes of hematite (α-Fe_2O_3)—(113), (024), and (116) as shown in Figure 2(c) through 2(e). The intensity of these peaks gradually increased for those com-CNT produced with the addition of atmospheric air, indicating that oxidation occurred more prevalently when oxygen from the air was introduced. However, the existence of α-Fe_2O_3 may have reduced the magnetic property of the composite products because the magnetization of α-Fe_2O_3 is lower than Fe_3O_4 [42]. The other new peaks also appeared at 18.05° and 19.81°, which correspond to (103) and (112) lattice planes of fullerenes C_{70} (#PDF 48-1206). The other observable peaks lower than 24°, were considered to be fullerenes or other carbon allotropes which have sp^2 hybridized carbon atom structures. In addition, the other crystalline planes of (002), (220), and (110) belonged to carbon and Fe_3C. The latter compound also contributed to the magnetic property of the CNT products.

To confirm the correlation between the representative data analyzed by the XRD with the other material characteristics, the product was next observed under electron microscopy to investigate the material structure, as shown in Figure 3. The TEM images in Figures 3(a-b), 3(c-d), and 3(e-f) show the com-CNT

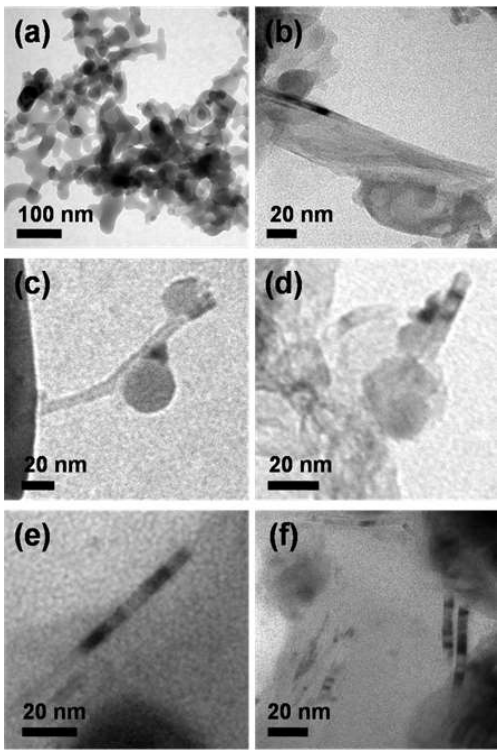

Figure 3. The TEM images of com-CNT produced in different pressure and gas condition; (a-b). 180 Torr with atmospheric air addition; (c-d). 100 Torr; and (e-f). 80 Torr without air addition.

synthesized using the CVD method in different pressure conditions of 80 Torr, without atmospheric air addition; 100 Torr, without atmospheric air addition; and 180 Torr, with atmospheric air addition, respectively.

As shown in Figure 3, the CNT formed under these three pressure conditions resulted in different forms. However, a magnetic particle of iron oxide was typically encased inside the CNT. These magnetic particles in the CNT structures derived magnetic properties to turn carbon nanotubes into magnetic com-CNT. Figure 3(a) shows the presence of iron oxide remaining from the catalyst used. Figure 3(b) shows the presence of CNT formed under 180 Torr pressure, with atmospheric air addition. The formation of com-CNT possibly occurred when the synthesis process was performed before the air was introduced to the chamber.

When synthesized in lower pressure conditions, com-CNT showed different patterns than those previously discussed, as presented in Figure 3(c-d), showing the presence of single-wall carbon nanotubes. The magnetic particles were observed attached on the CNT side, shown in Figure 3(c). This phenomenon was also observed in com-CNT by Georgakilas et al. (2005) [43] who synthesized their com-CNT in multiple steps of the co-precipitation method after the step of CNT preparation. In Figure 3(d), magnetic particles encased the CNT and were suggested to be in an agglomeration form.

Figure 3(e-f) shows the synthesized com-CNT produced in the lowest pressure studied in this research—80 Torr—at which the magnetic particles were also successfully encapsulated inside the CNT. However, the com-CNT growth was more straightly aligned. The encased metal catalyst inside the produced CNT was also observed in previously published pioneering works [31-34,44]. The com-CNT growth proceeds according to a sequence of steps: precursor diffusion in the chamber, precursor adsorption to the catalyst surface, the chemical reaction between the precursor and the catalyst, the formation of the resultant product with predominant carbon species, the desorption of the non-carbon product, the condensation of the carbon species in the bulk stream on the catalyst, and the arrangement of new chemical carbon bonds in hexagonal and/or pentagonal structures to form CNT [45]. There are two basic mechanisms of CNT growth reported during CVD processing, i.e., tip and base growth [11]. Considering the TEM images, the CNT growth mechanism produced in this study had mostly a tip growth shape, because the magnetic catalyst was encased in the middle of the CNT nearer the closed tip.

This difference possibly occurred because of the proposed mechanism of com-CNT formation—as illustrated in Figure 4—with the metal catalyst encapsulated in carbon produced by submerged arc discharge. In the proposed mechanism, the role of the catalyst, as both catalyst and carbon source, can be described in terms of CNT growth. CNT growth on the catalyst initiated the opening of the carbon shell where the core of iron compound was trapped inside. The opening of the carbon shell might be induced by oxidation caused by oxygen-containing species from the ethanol vapor or the air. The oxidation process led the double bonds in the carbon shell opened and connected to the other reactive carbon species to further self-assembly being hexagonal and/or pentagonal carbon structures. However, this oxidation process could completely oxidize the carbon shell when more oxygen oxidative species were introduced.

Therefore, in the experimental condition where CNT synthesized at higher pressure with air addition, the oxidation occurred more prevalently than in other synthesis conditions. The opening of the carbon shell, in the high-pressure case, was easier and higher, inducing the metal nanoparticles catalyst to begin coalescence, as shown in Figure 4. Due to the excessive oxidation, the carbon shell encapsulating the metal catalyst was completely oxidized, and the bare coalescence catalyst was formed. In the lower pressure condition without air addition, the particles coalescence also occurred. However the opening of the carbon shell, induced by oxidation, was lower than in the higher pressure experiment variation due to the limited oxygen-containing species, thus the carbon shell was not totally damaged. The CNT grew by opening the catalyst's carbon shell without coalescence might have been what happened in the lower pressure condition. This proposed condition was considered to depend on the fact that oxidation did

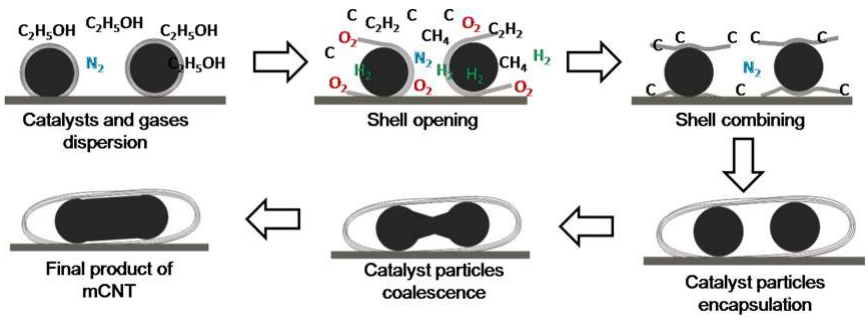

Figure 4. The growth mechanisms of com-CNT in CVD using carbon shell-catalyst core structure material.

not excessively occur to the catalyst, therefore, the catalyst crystal remained stable and unchanged—leading to the growth and arrangement of cluster particles inside the CNT.

This phenomenon of the attachment of the catalyst particles to the sides of the CNT (previously shown in Figure 3(c) probably happened to the bare catalyst particles which were not encapsulated inside the carbon shell. Therefore, because these nanoparticles were not surrounded by carbon, they attached outside the CNT rather than fill inside. These results propose that com-CNT in which the magnetic phase particles fill inside may be successfully synthesized only with carbon-encapsulated catalyst particles, the mechanisms for which are proposed in Figures 4.

The level of com-CNT magnetism was predicted from the interactions of the particles with a bar magnet. In Figure 5, com-CNT, produced in pressure conditions of 80 and 100 Torr, are shown to have had better interaction with magnets. This indicates that their magnetic levels are greater than that of com-CNT produced in pressure conditions of 180 Torr with added air. As shown in Figure 5(c), synthesis using ethanol vapor and atmospheric air resulted in a redder color than the other syntheses indicates to the phase transition of the iron oxide occurred after CVD treatment. At the high temperature set in this experiment, iron oxide easily reacted with oxygen and experienced oxidation. The existence of the oxygen which come from the ethanol vapor used in CVD as carbon source gas, led to the oxidation process. Additionally, the more oxygen species involved, the more oxidation process occurred; this was experienced on the catalyst treated in CVD at 180 torr with air addition. According to Kazeminezhad and Mosivand (2014) [46], the oxidation reactions of iron oxide can be shown in equations (1 " 2).

$$4Fe_3O_4 + O_2 \rightarrow 6\,(\gamma\text{-}Fe_2O_3) \quad \ldots\ldots. \quad (1)$$

$$4Fe_3O_4 + O_2 \rightarrow 6\,(\alpha\text{-}Fe_2O_3) \quad \ldots\ldots. \quad (2)$$

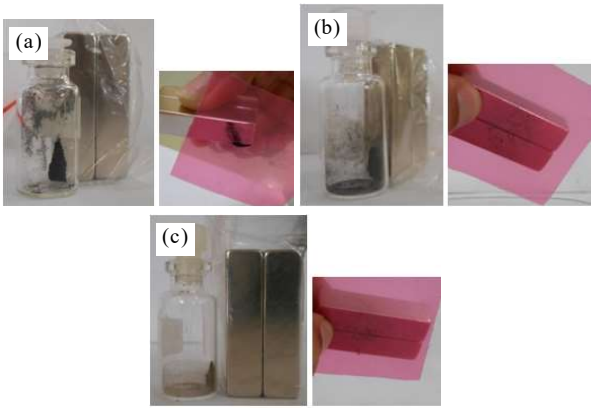

Figure 5. Magnetic interactions of com-CNT produced in different pressure and gas conditions; (a) 80 Torr and (b) 100 Torr without added atmospheric air; (c) 180 Torr with atmospheric air addition.

The formation of α-Fe_2O_3 caused the com-CNT magnetization to decrease, as indicated by the lower attraction of particles with the nearby magnet bar, as shown in Figure 5.

The com-CNT electrical resistance was roughly estimated by a LCR digital multimeter, as listed in Table 2. The higher electrical resistance belongs to the catalyst of iron oxide/carbon. The presence of iron oxide caused the value of the electrical resistance of com-CNT to rise. Carbon materials composed of iron oxide particles are, in general, less conductive, amorphous carbon. Thus, they have a larger electrical resistance value. As shown in Table 2, the pristine catalyst of Fe_3O_4/carbon has the highest electrical resistance. The smallest electrical resistance was obtained from com-CNT produced at 100 Torr without added atmospheric air, which was equal to 18.9 Ω. The com-CNT produced at this Torr pressure also had the highest magnetic levels. On the other hand, com-CNT produced at 180 Torr with added atmospheric air had the highest electrical resistance of 89.0 Ω and also had lower magnetic levels. Therefore, the measured electrical resistance was inversely proportional to the material's magnetic level, and the magnetism of the carbon nanomaterial produced in this study is inversely proportional to electrical conductivity. The com-CNT produced at 180 Torr with added atmospheric air had the highest electrical resistance value, due to the excessive oxidation process caused by the atmospheric air. The com-CNT produced in lower pressure conditions had lower electrical resistance values.

Table 2. fgdfjghdfgisufsiufsiud iursiee siursieh siursierh uiserse uierser uierse r9

Material	R(Ω)	Magnetism#
Graphite	7.6 ± 0.1	-
Iron oxide (Fe_3O_4)	OL*	+++++
Fe_3O_4/carbon	132.2 ± 0.1	+++
mCNT (180 torr +air)	89.0 ± 0.1	+
mCNT(100 torr)	18.9 ± 0.1	++
mCNT (80 torr)	55.1 ± 0.1	++++

*OL (over load)
The magnetism level as labeled by '+' was roughly observed from the material attraction to a magnet bar. More '+' indicate to the higher magnetic response

CONCLUSION

The formation of com-CNT was determined by the shifted X-ray diffracted peak of carbon C(002), the presence of peaks from the iron oxides Fe_3O_4 and γ-Fe_2O_3, and the formation of other peaks highly considered to belong to other carbon allotropes with sp^2 hybridization structures. The com-CNT synthesized in CVD using the iron oxide/carbon catalyst were successfully observed by TEM, showing the presence of single-wall carbon nanotubes. These carbon nanotubes had a magnetic property, which was induced by the metal catalyst remaining inside the CNT. The measured electrical

resistance was inversely proportional to the material's magnetism. The com-CNT produced in lower pressure (100 Torr) conditions revealed lower electrical resistance and better magnetic response. Overall, this work's synthesized com-CNT produced using CVD have better electrical performance compared to the pristine catalyst of iron oxide/carbon.

ACKNOWLEDGMENT

This work was partly supported by Grants-in-Aid Research from the Ministry of Research, Technology and Higher Education, under project No. 474/UN27.21/PP/2018 and 718/UN27.21/PN/2019.

REFERENCES

[1]. Iijima, S., Helical microtubules of graphitic carbon. *Nature*, 354(6348), pp. 56-58, 1991.

[2]. Dillon, F.C., Moghal, J., Koós, A., Lozano, J.G., Miranda, L., Porwal, H., Reece, M.J., & Grobert, N., Ceramic composites from mesoporous silica coated multi-wall carbon nanotubes. *Microporous and Mesoporous Materials*, 217159-166, 2015.

[3]. Ma, Y., Sheng, L., Zhao, H., An, K., Yu, L., Xu, J., & Zhao, X., Synthesis of NiO/carbon shell/single-walled carbon nanotube composites as anode materials for lithium ion batteries. *Solid State Sciences*, 4649-55, 2015.

[4]. Chang-Jian, S.-K., Ho, J.-R., & John Cheng, J.W., Fabrication of transparent double-walled carbon nanotubes flexible matrix touch panel by laser ablation technique. *Optics & Laser Technology*, 43(8), pp. 1371-1376, 2011.

[5]. Ando, Y., & Zhao, X., Synthesis of carbon nanotubes by arc-discharge method. *New Diamond and Frontier Carbon Technology*, 16(3), pp. 123-138, 2006.

[6]. ChandraKishore, S., & Pandurangan, A., Synthesis and characterization of Y-shaped carbon nanotubes using Fe/AlPO4 catalyst by CVD. *Chemical Engineering Journal*, 222472-477, 2013.

[7]. Hofmann, S., Kleinsorge, B., Ducati, C., Ferrari, A.C., & Robertson, J., Low-temperature plasma enhanced chemical vapour deposition of carbon nanotubes. *Diamond and Related Materials*, 13(4), pp. 1171-1176, 2004.

[8]. Wilson, J.I.B., Scheerbaum, N., Karim, S., Polwart, N., John, P., Fan, Y., & Fitzgerald, A.G., Low temperature plasma chemical vapour deposition of carbon nanotubes. *Diamond and Related Materials*, 11(3), pp. 918-921, 2002.

[9]. Choi, C.H., Lee, S.Y., Park, S.H., & Woo, S.I., Highly active N-doped-CNTs grafted on Fe/C prepared by pyrolysis of dicyandiamide on Fe2O3/C for electrochemical oxygen reduction reaction. *Applied Catalysis B: Environmental*, 103(3–4), pp. 362-368, 2011.

[10]. Koziol, K., Boskovic, B.O., & Yahya, N., *Synthesis of Carbon Nanostructures by CVD Method*. in: N. Yahya, ed., Carbon and Oxide Nanostructures: Synthesis, Characterisation and Applications, Springer Berlin Heidelberg, Berlin, Heidelberg, pp. 23-49. 2011.

[11]. Kumar, M., & Ando, Y., Chemical Vapor Deposition of Carbon Nanotubes: A Review on Growth Mechanism and Mass Production. *Journal of Nanoscience and Nanotechnology*, 10(6), pp. 3739-3758, 2010.

[12]. Moshkalyov, S.A., Moreau, A.L.D., Guttiérrez, H.R., Cotta, M.A., & Swart, J.W., Carbon nanotubes growth by chemical vapor deposition using thin film nickel catalyst. *Materials Science and Engineering: B*, 112(2–3), pp. 147-153, 2004.

[13]. Du, C., & Pan, N., CVD growth of carbon nanotubes directly on nickel substrate. *Materials Letters*, 59(13), pp. 1678-1682, 2005.

[14]. Lee, O., Jung, J., Doo, S., Kim, S.-S., Noh, T.-H., Kim, K.-I., & Lim, Y.-S., Effects of temperature and catalysts on the synthesis of carbon nanotubes by chemical vapor deposition. *Metals and Materials International*, 16(4), pp. 663-667, 2010.

[15]. Bistamam, M.S.A., & Azam, M.A., Tip-growth of aligned carbon nanotubes on cobalt catalyst supported by alumina using alcohol catalytic chemical vapor deposition. *Results in Physics*, 4105-106, 2014.

[16]. Chiangga, S., Suttisiri, N., & Nilsaengrat, P., Effect of temperature on carbon nanotubes growth on thin Iron film by thermal chemical vapor deposition method under the low pressure. *Physics Procedia*, 2(1), pp. 107-111, 2009.

[17]. Sun, L.F., Mao, J.M., Pan, Z.W., Chang, B.H., Zhou, W.Y., Wang, G., Qian, L.X., & Xie, S.S., Growth of straight nanotubes with a cobalt–nickel catalyst by chemical vapor deposition. *Applied Physics Letters*, 74(5), pp. 644-646, 1999.

[18]. Lee, S.-F., Chang, Y.-P., & Lee, L.-Y., Synthesis of carbon nanotubes on silicon nanowires by thermal chemical vapor deposition. *New Carbon Materials*, 26(6), pp. 401-407, 2011.

[19]. Liu, W.-W., Aziz, A., Chai, S.-P., Mohamed, A.R., & Hashim, U., Synthesis of Single-Walled Carbon Nanotubes: Effects of Active Metals, Catalyst Supports, and Metal Loading Percentage. *Journal of Nanomaterials*, 20138, 2013.

[20]. Osorio, A.G., Machado, G.B., Pereira, M.B., Benvenutti, E.V., Pereira, L.G., Bergmann, C.P., Oliveira, A.H.d., & Costa, T.M.H., Synthesis and characterization of magnetic carbon nanotubes/silsesquioxane nanocomposite thin films. *Applied Surface Science*, 3719-15, 2016.

[21]. Kuemmeth, F., Churchill, H.O.H., Herring, P.K., & Marcus, C.M., Carbon nanotubes for coherent spintronics. *Materials Today*, 13(3), pp. 18-26, 2010.

[22]. Gao, C., Li, W., Morimoto, H., Nagaoka, Y., & Maekawa, T., Magnetic Carbon Nanotubes: Synthesis by Electrostatic Self-Assembly Approach and Application in Biomanipulations. *The Journal of Physical Chemistry B*, 110(14), pp. 7213-7220, 2006.

[23]. Jia, B., Gao, L., & Sun, J., Self-assembly of magnetite beads along multiwalled carbon nanotubes via a simple hydrothermal process. *Carbon*, 45(7), pp. 1476-1481, 2007.

[24]. Sowichai, K., Supothina, S., Nimittrakoolchai, O.-u., Seto, T., Otani, Y., & Charinpanitkul, T., Facile method to prepare magnetic multi-walled carbon nanotubes by in situ co-precipitation route. *Journal of Industrial and Engineering Chemistry*, 18(5), pp. 1568-1571, 2012.

[25]. Mishra, A.K., & Ramaprabhu, S., Magnetite Decorated Multiwalled Carbon Nanotube Based Supercapacitor for Arsenic Removal and Desalination of Seawater. *The Journal of Physical Chemistry C*, 114(6), pp. 2583-2590, 2010.

[26]. Yang, Z.-F., Li, L.-Y., Hsieh, C.-T., & Juang, R.-S., Co-precipitation of magnetic Fe3O4 nanoparticles onto carbon nanotubes for removal of copper ions from aqueous solution. *Journal of the Taiwan Institute of Chemical Engineers*, 8256-63, 2018.

[27]. Xiao, D., Dramou, P., He, H., Pham-Huy, L.A., Li, H., Yao, Y., & Pham-Huy, C., Magnetic carbon nanotubes: synthesis by a simple solvothermal process and application in magnetic targeted drug delivery system. *Journal of Nanoparticle Research*, 14(7), pp. 984, 2012.

[28]. Wu, H., Liu, G., Wang, X., Zhang, J., Chen, Y., Shi, J., Yang, H., Hu, H., & Yang, S., Solvothermal synthesis of cobalt ferrite nanoparticles loaded on multiwalled carbon nanotubes for magnetic resonance imaging and drug delivery. *Acta Biomaterialia*, 7(9), pp. 3496-3504, 2011.

[29]. Guan, Y., Jiang, C., Hu, C., & Jia, L., Preparation of multi-walled carbon nanotubes functionalized magnetic particles by sol–gel technology and its application in extraction of estrogens. *Talanta*, 83(2), pp. 337-343, 2010.

[30]. Zhang, X.X., Wen, G.H., Huang, S., Dai, L., Gao, R., & Wang, Z.L., Magnetic properties of Fe nanoparticles trapped at the tips of the aligned carbon nanotubes. *Journal of Magnetism and Magnetic Materials*, 231(1), pp. 9-12, 2001.

[31]. Korneva, G., Ye, H., Gogotsi, Y., Halverson, D., Friedman, G., Bradley, J.-C., & Kornev, K.G., Carbon Nanotubes Loaded with Magnetic Particles. *Nano Letters*, 5(5), pp. 879-884, 2005.

[32]. Sengupta, J., Jana, A., Pradeep Singh, N.D., Mitra, C., & Jacob, C., Site-selective synthesis of in situ Ni-filled multi-walled carbon nanotubes using Ni(salen) as a catalyst source. *Nanotechnology*, 21(41), pp. 415605, 2010.

[33]. Zeeshan, M.A., Shou, K., Pané, S., Pellicer, E., Sort, J., Sivaraman, K.M., Baró, M.D., & Nelson, B.J., Structural and magnetic characterization of batch-fabricated nickel encapsulated multi-walled carbon nanotubes. *Nanotechnology*, 22(27), pp. 275713, 2011.

[34]. Baro, M., & Pal, A.R., One-step grown multi-walled carbon nanotubes with Ni filling and decoration. *Journal of Physics D: Applied Physics*, 48(22), pp. 225303, 2015.

[35]. Bekarevich, R.V., Miura, S., Ogino, A., Rahachou, A.U., & Nagatsu, M., The Effect of Substrate on the Low-Temperature Carbon Nanomaterials Growth by Microwave Excited Surface-wave Plasma Chemical Vapor Deposition. *Journal of Physics: Conference Series*, 417(1), pp. 012042, 2013.

[36]. Saraswati, T.E., Prasiwi, O.D.I., Masykur, A., Handayani, N., & Anwar, M., The Modification of Carbon with Iron Oxide Synthesized in Electrolysis Using the Arc Discharge Method. *IOP Conference Series: Materials Science and Engineering*, 176(1), pp. 012046, 2017.

[37]. Celzard, A., Marêché, J.F., Payot, F., & Furdin, G., Electrical conductivity of carbonaceous powders. *Carbon*, 40(15), pp. 2801-2815, 2002.

[38]. Saraswati, T.E., Retnosari, I., Hayati, I.N., Amalia, A., & Hastuti, S., The Influence of Ammonia Addition on the Surface Characteristics of Fe3O4/ Carbon Nanoparticles in Submerged Arc Discharge. *Recent Patents on Materials Science*, 11(2), pp. 71-82, 2018.

[39]. Zhang, L., Ni, Q.-Q., Natsuki, T., & Fu, Y., Carbon nanotubes/magnetite hybrids prepared by a facile synthesis process and their magnetic properties. *Applied Surface Science*, 255(20), pp. 8676-8681, 2009.

[40]. Sun, Z., Liu, Z., Wang, Y., Han, B., Du, J., & Zhang, J., Fabrication and characterization of magnetic carbon nanotube composites. *Journal of Materials Chemistry*, 15(42), pp. 4497-4501, 2005.

[41]. Song, K., Lee, S., Suh, C.-Y., Kim, W., Ko, K.-S., & Shin, D., Synthesis and Characterization of Iron Oxide Nanoparticles Prepared by Electrical Explosion of Fe Wire in Ar-O_2 Gas Mixtures *Materials Transactions*, 53(11), pp. 4, 2012.

[42]. Patimah, P., & Saraswati, T.E., Pengaruh Suhu Kalsinasi Pada Sifat Kemagnetan Material Besi Oksida Hasil Elektrolisis. *Jurnal Kimia dan Pendidikan Kimia*, 1(3), pp. 149-156, 2016.

[43]. Georgakilas, V., Tzitzios, V., Gournis, D., & Petridis, D., Attachment of Magnetic Nanoparticles on Carbon Nanotubes and Their Soluble Derivatives. *Chemistry of Materials*, 17(7), pp. 1613-1617, 2005.

[44]. Qu, S., Huang, F., Yu, S., Chen, G., & Kong, J., Magnetic removal of dyes from aqueous solution using multi-walled carbon nanotubes filled with Fe2O3 particles. *Journal of Hazardous materials*, 160(2), pp. 643-647, 2008.

[45]. Meyyappan, M., Delzeit, L., Cassell, A., & Hash, D., Carbon nanotube growth by PECVD: a review. *Plasma Sources Science and Technology*, 12(2), pp. 205-216, 2003.

[46]. Kazeminezhad, I., & Mosivand, S., Phase transition of electrooxidized Fe3O4 to γ and α-Fe2O3 nanoparticles using sintering treatment. *Acta Physica Polonica A*, 125(5), pp. 1210-1214, 2014.